# LUMINOUS-INTENSITY MEASUREMENTS OF SOURCES USING A NEW DETECTOR-BASED ILLUMINANCE SCALE

George Eppeldauer, Christopher L. Cromer, and Jonathan E. Hardis

Radiometric Physics Division
National Institute of Standards and Technology
U. S Department of Commerce – Technology Administration
Gaithersburg, Maryland 20899

Abstract.

Until recently, the source-based photometric scale of NIST had been derived from the gold-point black-body using a long derivation chain resulting in a scale uncertainty of about 1%. In order to improve the accuracy of the photometric scale, a new detector-based illuminance scale has been realized with an uncertainty about twice as small as that of the previous source-based scale. The realization of the new illuminance scale was made by photometers calibrated for absolute spectral response, traceable to NIST primary standard detectors using a short derivation chain. The luminous intensity scale is derived from the illuminance scale.

With the introduction of the new photometric scale, the photometric calibration services of NIST will include luminous intensity and luminance calibration of different kinds of light sources, measured with standard photometers. Luminous intensity measurements of LEDs are discussed as an example to illustrate the new calibration services. In addition, the new photometric scale will allow calibration of illuminance and luminance meters with standard photometers, using different kinds of light sources.

Keywords: calibration, candela, detector, illuminance, light source, luminance, luminous flux, luminous intensity, lumen, lux, photometry, standard

## 1. Introduction.

In 1979 the photometric base unit, the candela, was redefined as follows:

> The candela is the luminous intensity, in a given direction, of a source that emits monochromatic radiation of frequency $540\times10^{12}$ Hz and that has a radiant intensity in that direction of 1/683 W/sr [1].

According to this definition, photometric quantities are directly related to radiometric quantities. The radiant power at different wavelengths is weighted according to the spectral responsivity of the human visual system. The weighting function for photopic vision is $V(\lambda)$, which peaks at a value of 1 at 555 nm [2], near the corresponding wavelength of the $540\times10^{12}$ Hz frequency in the definition.



0-8194-0852-2/92/$4.00

Until recently, the luminous intensity scale at NIST was derived from the NIST spectral irradiance scale using gas-filled, inside-frosted tungsten lamps. The spectral irradiance scale is derived from the spectral radiance scale, which is based on the spectral radiance of a gold-point black-body. Because of the many derivation steps and the drift of lamps, the reported uncertainty of the source-based NIST photometric scale was 1.0% ($3\sigma$) with respect to the definition of the SI unit. The reported long term reproducibility was 0.8% ($3\sigma$) [3].

However, the candela redefinition in 1979 allowed for additional methods of realizing a photometric scale. Not only national laboratories [4, 5], but also small research facilities [6] have taken advantage of these possibilities. It was common that either absolute radiometers or spectrally calibrated silicon photodiodes were equipped with photopic correcting filters. Different kinds of absolute radiometers were used: a cryogenic electrical substitution radiometer with silicon photodiode transfer standards [4], electrically calibrated thermal detectors [5], and self-calibrated silicon photodiodes [6, 7, 8].

Today, a group of eight photometers has been developed at NIST for the measurement of photometric quantities and to realize the candela. The characterization and the calibration of these photometers are discussed in detail in reference [9]. Each photometer includes a silicon photodiode radiometer with a limit sensitivity of 3 fW at 555 nm, when the electrical bandwidth is 0.3 Hz. The spectral responsivity of the silicon photodiode radiometer is modified with a $V(\lambda)$ matching filter. The photometric limit sensitivity is $4\times10^{-7}$ lx. This high sensitivity for filter-corrected radiometers is an important requirement for a calibration precision of better than 0.1% in the wings of the $V(\lambda)$ curve, where the signal is very small [10, 11, 12]. This paper discusses the application of these standard devices.

## 2. The Detector Based Photometric Scale.

The candela is derived from the photometric equivalent of the radiant power, called luminous flux, $\Phi$, which is to be measured by the photometer:

$$\Phi = K_m \int_\lambda N(\lambda)\, V(\lambda)\, d\lambda \quad [\mathrm{lm}] \qquad (1)$$

where $K_m = 683$ lm/W, the maximum luminous efficacy, $N(\lambda)$ is the incident radiant power, and $V(\lambda)$ is the CIE spectral luminous efficiency function for photopic vision. The illuminance responsivity [13] of the standard photometer, S, is given by:

$$S = \frac{I\,Z}{\Phi} = \frac{s(555)\,Z}{K_m\,F} \quad [\mathrm{A/lx}] \qquad (2)$$

where I is the output current of the photometer, Z is the aperture area, s(555) is the absolute response at 555 nm, and lx=lm/m$^2$. F in equation (2) is the correction factor for the spectral mismatch, for a given light source, of the relative spectral responsivity of the photometer $s_n(\lambda)$ (normalized to 1 at 555 nm) to the $V(\lambda)$ function:

$$F = \frac{\int_\lambda V(\lambda)\, N(\lambda)\, d\lambda}{\int_\lambda s_n(\lambda)\, N(\lambda)\, d\lambda} \quad . \qquad (3)$$

The luminous intensity of a light source, C, can be calculated from the measured output current I of a photometer:

$$C = \frac{K_m F I}{s(555)\, Z}\, D^2 \ [cd] \qquad (4)$$

where D is the distance between the source and the limiting precision aperture of the photometer. Equation (4) is valid if D is large enough for the source to act as a point source.

3. Construction of the Photometers.

The three basic components, the silicon photodiode, the $V(\lambda)$ correcting filter, and the precision aperture, are mounted in the front piece of a cylindrical housing, as shown in Fig. 1. The photodiode is plugged into a socket with a teflon base of high electrical resistance. The $V(\lambda)$ filter package is glued into a filter holder and is positioned close to the photodiode. In front of the filter package, the precision aperture is glued to the reference surface of the aperture holder. The distance of this reference surface to the front surface of the housing is 3.00 mm for each photometer. A marking system was used so that the photometer could be disassembled and reassembled in the same manner. The temperature of the assembly is monitored with a temperature sensor, mounted in the wall of the front piece of the housing [14].

The electronic assembly is in the cylindrical housing, under the front piece described above. It consists of a current to voltage converter [9] and the electronic circuit for the temperature sensor. The two analog outputs, a seven or eight decade sensitivity switch, and a cable to the DC power supply are mounted on the back panel of the cylindrical housing. The housing is light-tight and electrically shielded.

4. Characterization of the Photometers.

The silicon photodiodes and the photopic filters were characterized spectrally and spatially in order to select the best samples from a larger group, and to monitor changes in each component with time. We used silicon photodiodes with large active areas (0.3 $cm^2$ to 1.0 $cm^2$) and quartz windows. Selection of the best filters to minimize non-uniformity was necessary, because spatial non-uniformity of filter transmittance as high as 1% was common among filters of the same batch. The uniformity of the combined package was then measured at 50 nm intervals from 400 nm to 750 nm.

To check the blocking of the filters outside the visible range, the residual UV and IR leakage was measured between 200 to 380 nm and 780 to 1100 nm, respectively. The infrared response of

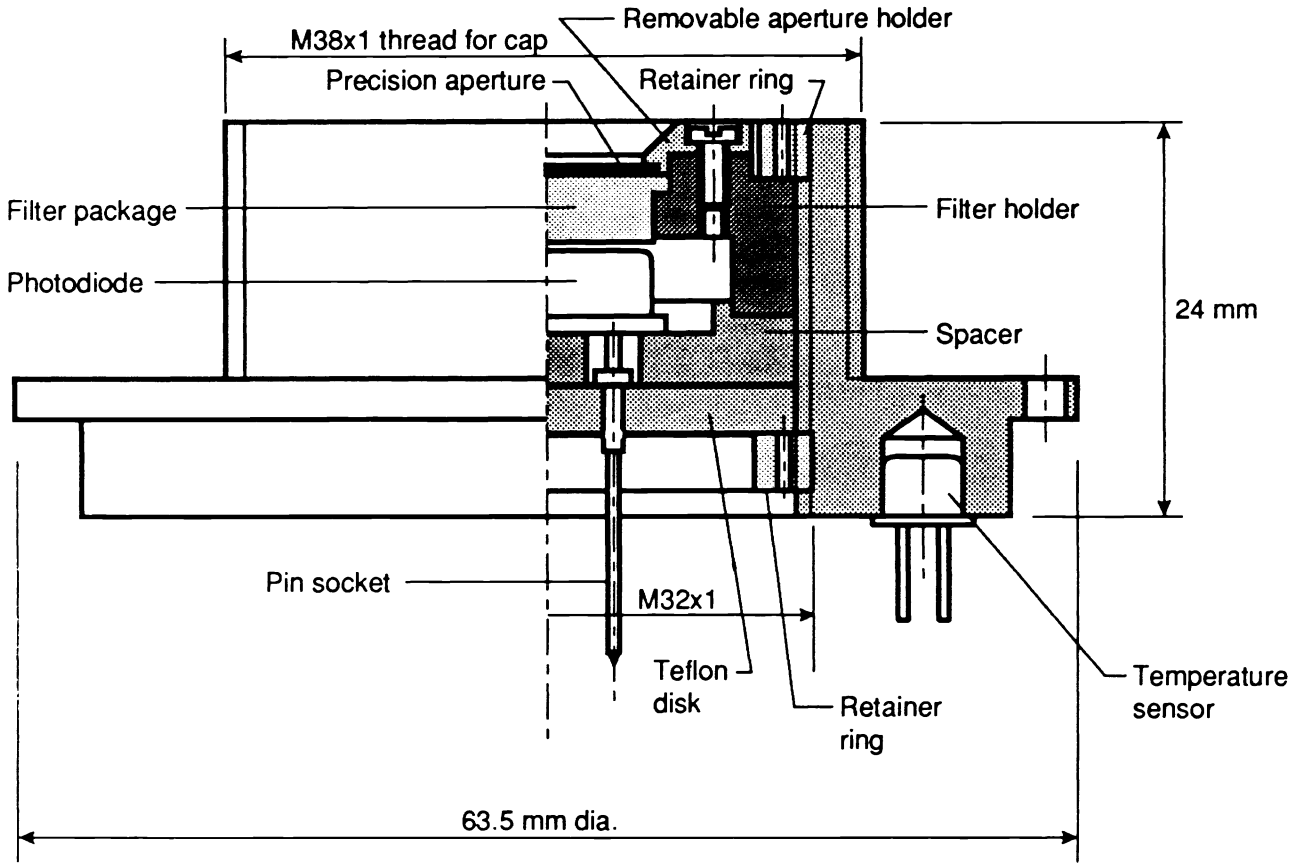


Fig. 1.
Photometer construction.

each photometer was less than 0.003% of the signal for a standard illuminant A source. The UV response was less than 0.002%.

The temperature dependence of the photometers was determined by making measurements of the photometer response with a constant illuminance as the temperature was increased. The largest temperature dependence measured was 0.088% /°C.

The photocurrent-to-voltage converter electronics are described in detail elsewhere [9]. In summary, the output drift with changing temperature is less than 12 fA (equivalent photocurrent) per degree (K). The noise floor is 1 fA (equivalent photocurrent) for integration times of 1.67 s. The settling time is 2 minutes on the $10^{11}$ V/A gain range, 1 s on the $10^{10}$ V/A range, and negligible on less sensitive ranges. The exact current-to-voltage conversion factor is determined with a precision current source for each gain range relative to the gain range used during the radiometric calibrations.

The assembled detector-filter-aperture packages were calibrated for absolute spectral response. The advantage of this method is that the internal reflections and scattering of the components in the photometers are the same during calibration and measurement. Calibration of the photometers for absolute spectral response was made on the NIST Spectral Comparator [15]. The calibration procedure and the uncertainty budget of the new detector based illuminance scale is published elsewhere [16, 17]. The overall uncertainty of the new illuminance scale is 0.5% ($3\sigma$).

The spectral mismatch correction factor, F, was calculated for each photometer presuming the spectral power distribution $N(\lambda)$ of the CIE standard illuminant A source (2856 K). The F value was 0.9997 for the best and 0.9538 for the worst filter match to the $V(\lambda)$ function. From these, the photometric luminous flux responsivities were calculated. Using an aperture with a nominal area of 0.1 $cm^2$, the illuminance responsivity of the photometers was typically 2.4 nA/lx. When used with a nominal amplifier gain of $10^7$ V/A, the photometers had a typical response of 24 mV/lx.

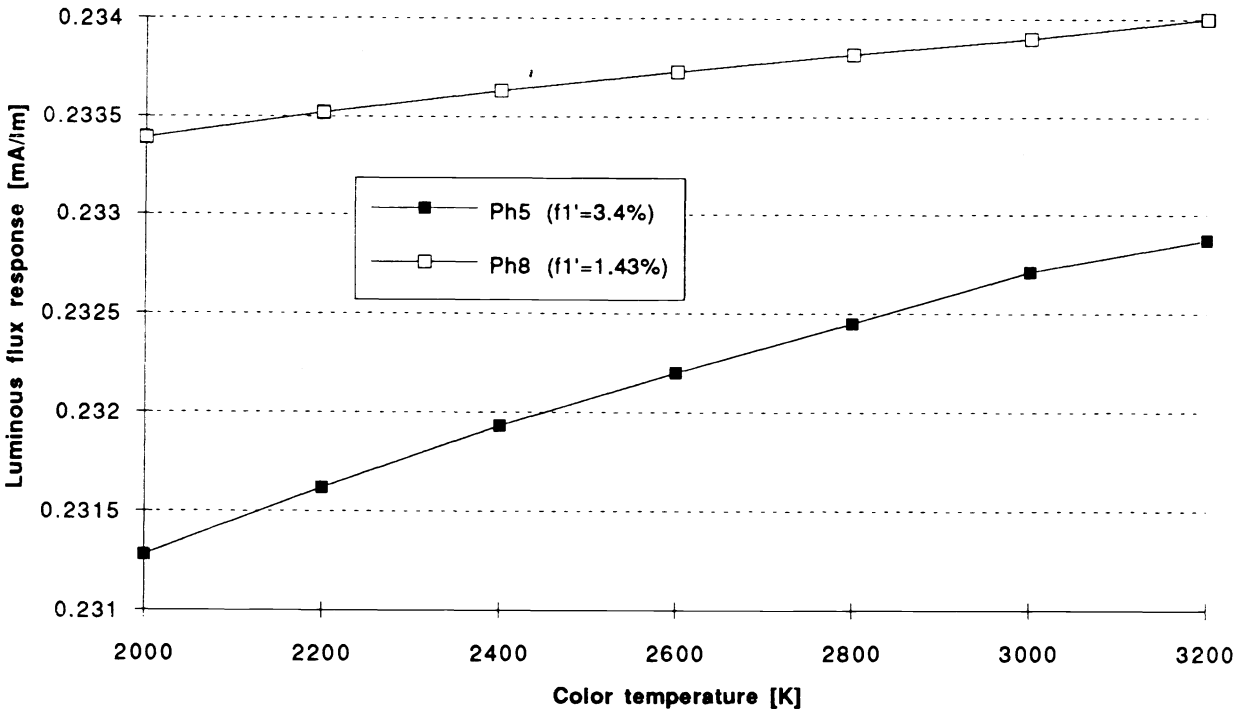


Fig. 2.
Photometric responses of photometer #5 and #8 as function of color temperature.

Fig. 2 shows the photometric response for other color temperatures, due to the different calculated F values. According to the CIE, $f_1'$ is the closeness with which the relative spectral responsivity of a photometer matches the $V(\lambda)$ function [18]. This was 1.43% for the better and 3.4% for the other photometer. The better the spectral match of the photometer to the $V(\lambda)$ function, the smaller

the change of the photometric responsivity for different color temperatures. For the best accuracy, F should be calculated using the actual power distribution of the source.

5. Utilization of the Standard Photometers.

The standard photometers normally measure illuminance. Additional photometers can be calibrated for illuminance responsivity (A/lx), as it is defined in eq. 2, by comparing them with the standards, using direct substitution with the same light source at a number of different distances. During such illuminance calibrations, the short-term stability of the source has to be high enough to keep it from becoming a significant factor in the uncertainty budget. Alternatively, the source intensity can be independently monitored and compensated.

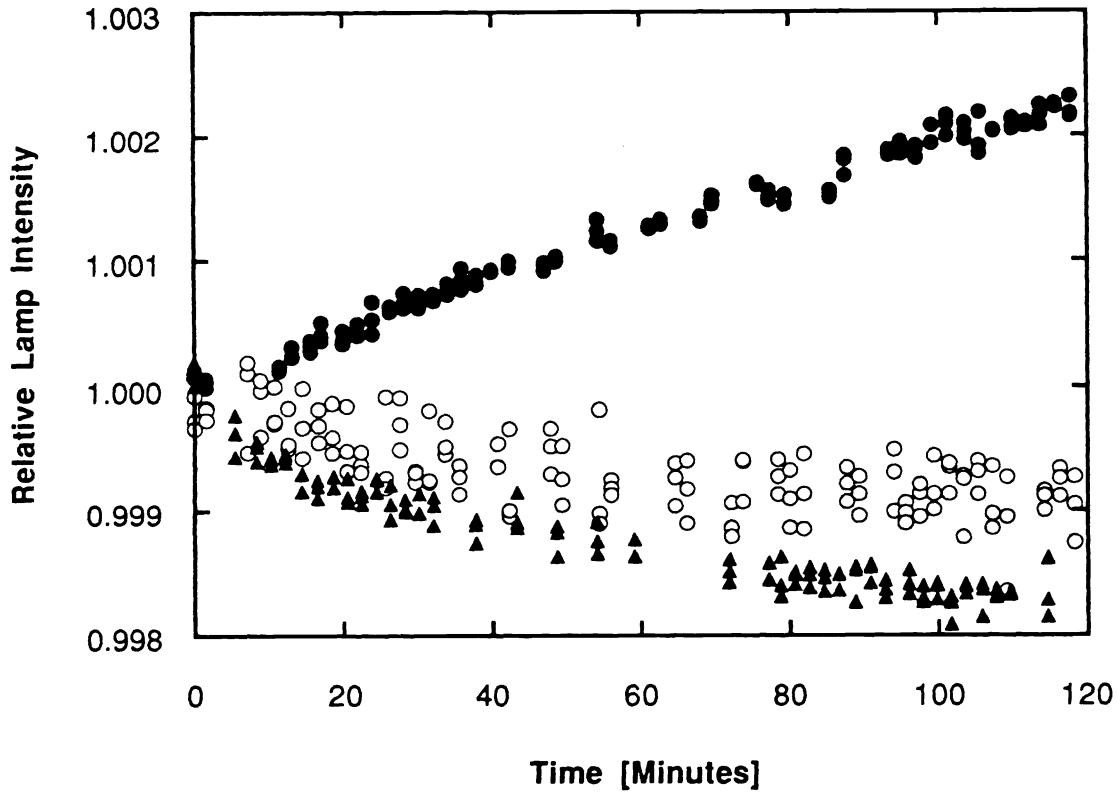


Fig. 3
Short term drift of standard lamps. Upper: Osram Wi 41/G; Middle: 1000W FEL; Lower: 500 W inside frosted T-20 lamp.

Short-term relative lamp intensity changes of three different kinds of lamps were measured on the NIST photometric bench. The results, shown in Fig. 3, indicated that monitoring and compensation would be appropriate. A monitor detector was constructed which incorporated a temperature-controlled silicon photodiode. The proper positioning of the monitor detector was

important because the intensity changes of the lamps were different in different directions. When the monitor detector was close to the lamp and far from the optical axis, the drift and noise did not correlate with that from the on axis photometer, as shown in Fig. 4. When the monitor was close to the axis and nearly the same distance from the lamp, both signals tracked together, as shown in Fig. 5.

The luminous intensity of a source can be calculated using equation 4. (The distance between the source and the photometer is measured using a precision electronic ruler on the NIST photometer bench [16]). The luminous intensities of a group of five inside-frosted lamps were measured with the eight standard photometers. Each lamp was measured with all eight photometers in quick succession during one lighting under the same conditions. The repeatability of the measurements from a set of eight remeasurements was 0.02%. The random errors that arose during the absolute spectral response calibrations and the illuminance measurements caused some photometers to measure illuminances that were consistently higher or lower than the others. The overall variation was approximately 0.15% of the mean. However, after correcting individual assignments to remove the pattern of offsets (while maintaining the group average) the variation of results among the photometers for a single lamp was reduced to typically 0.06%.

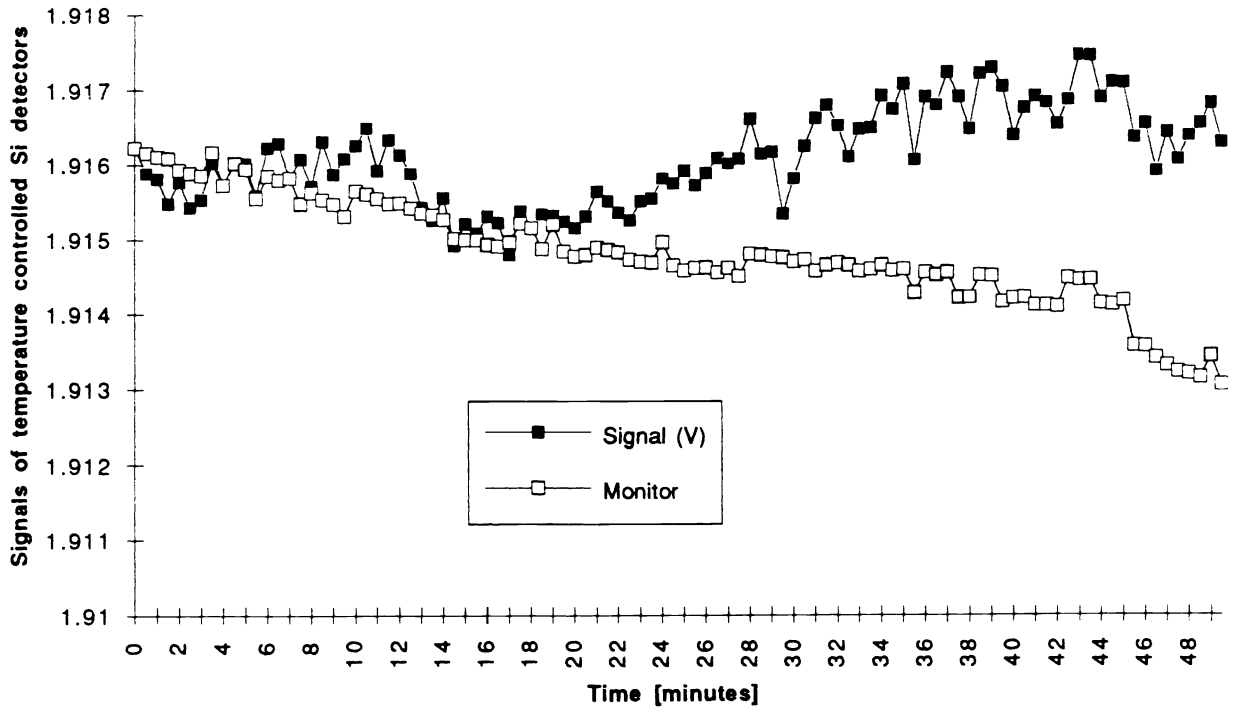


Fig. 4.

Intensity changes of a 500W inside frosted T-20 lamp in different directions. The photometer is in the optical axis of the photometric bench, far from the lamp. The monitor detector is close to the lamp and far from the optical axis.

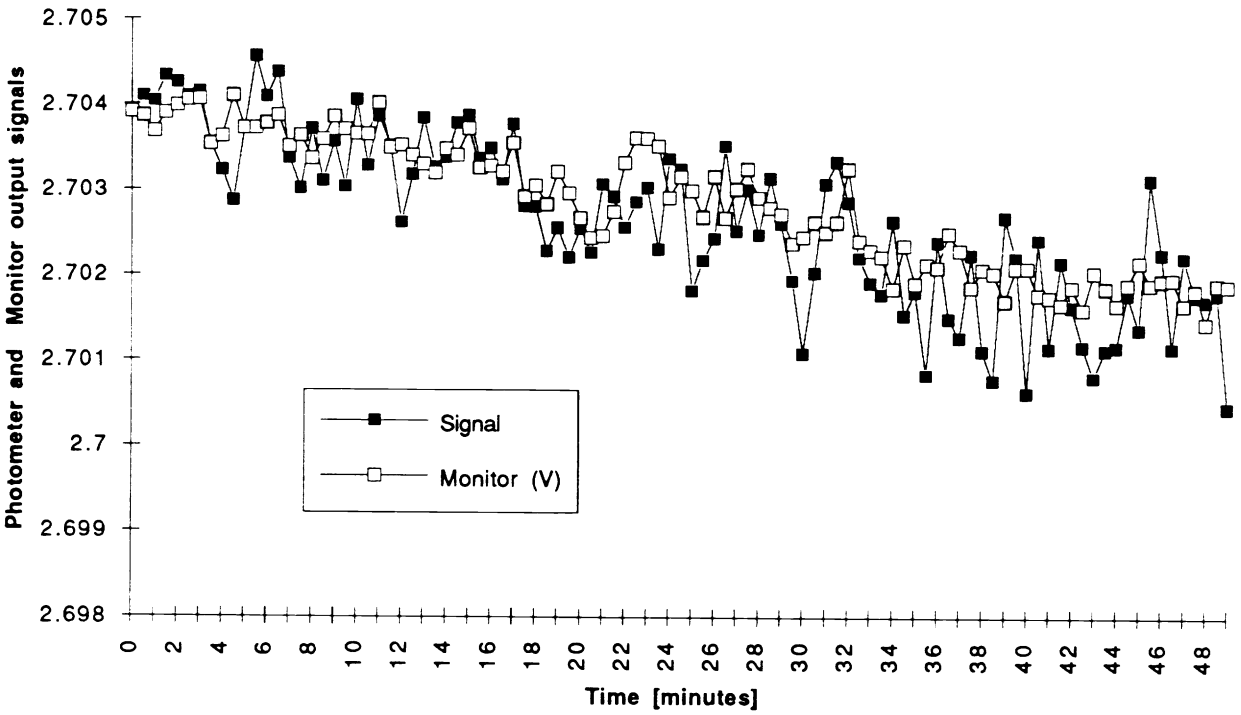


Fig. 5.
Intensity changes of a 500W inside frosted T-20 lamp. The monitor is close to the optical axis of the photometric bench and far enough from the lamp.

The 0.65% reported uncertainty of the luminous intensity scale [17] includes the 0.56% uncertainty of the detector-based illuminance scale and a 0.1% uncertainty estimate because of the short-term intensity changes of the standard lamps (the components were combined in quadrature). It also includes a 0.35% uncertainty in the lamp-to-aperture distance measurement, D in equation (4). This uncertainty is caused by the difference in position between the "effective origin" of the light and the mechanical center of the lamp. The distance to the effective origin can be determined by making illuminance measurements at many distances and by applying the inverse-square law. The offset between the effective and the geometric centers depends not only on the lamp type, it also varies between individual lamps of the same type. A 0.35% systematic uncertainty corresponds to a 6.5 mm shift of the light origin at a distance of 3.7 m, which was the most severe offset noted on several inside frosted lamps. In routine luminous intensity calibrations the geometrical center of the inside frosted lamps is used, and such a potential systematic error is anticipated.

A luminance scale can be derived from the illuminance scale by measuring the illuminance due to a uniform large-area source with known aperture size at a measured distance. We plan to calibrate the exit port of an integrating sphere, illuminated by a tungsten lamp, using the standard photometers. Luminance meters can then be calibrated using the sphere source. The sphere source can also be used with other types of light sources, and luminance meters can be calibrated with

these other source distributions. Of course, the F factors for the photometers would have to be recomputed for each distribution.

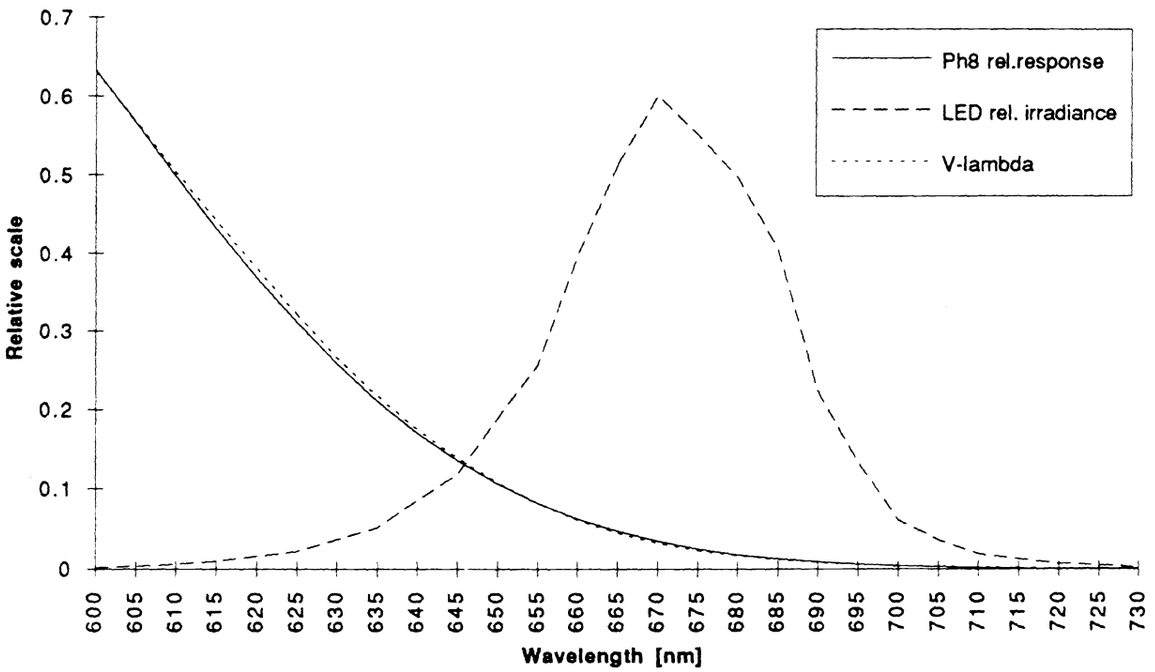


Fig. 6.
Photometer's spectral response and average spectral irradiance of the measured LEDs

Light emitting diodes (LEDs) emit much lower light levels than standard lamps, and their emission is confined to a narrow wavelength band of the visible spectrum. Nevertheless, the high-sensitivity standard photometers proved suitable for measuring their luminous intensity as well. The luminous intensities of lens free LEDs were measured with photometer #8 at three different distances on the NIST photometric bench. A nominal 2 m distance was used, which was long enough to apply the inverse square law and to neglect the small distance between the front surface and the radiating chip of the LEDs. The signal to noise ratio was 500:1 at a nominal luminous intensity of 2 mcd. In some cases, LEDs have a rapidly varying angular light distribution. This is why the $3\sigma$ repeatability of our LED luminous intensity calibrations (1%) was not as good as with tungsten lamps.

We used the standard photometer with the best spectral match to the CIE $V(\lambda)$ luminous efficiency function. $f_1'$ was 1.43%. This small value meant a very good spectral match, even in the narrow wavelength range of the LEDs.

As a first approximation, the standard responsivity assignment for the photometer was used. F was 0.9997, as computed assuming CIE Standard Illuminant A. However, photometric accuracy

depends on computing the F factor using the actual source spectrum. The relative spectral power distributions of the LEDs were measured on the FASCAL at NIST [19] in 10 nm steps. The peak emission wavelength was 670 nm for all LEDs. The emitting wavelength range was generally 620 to 720 nm. (The responsivity of the photometer in that spectral range had previously been determined.) The magnified wing of the photometer's relative spectral response curve, the CIE $V(\lambda)$ curve, and the average relative irradiance of the LEDs are shown in Fig. 6. Using this data, F was recalculated (equation (3)) to be 1.013. The revised F caused the initial results to be reduced by 1.3% (equation (4)), even with the photometer's excellent spectral match.

Acknowledgments.

The authors would like to extend thanks to Hong Sun for her participation in the radiometric characterizations, to Tom Larason for the absolute spectral response measurements, and to Al Parr for his technical advice and support.

References.

1. Monograph of the Bureau International des Poids et Measures (BIPM): Principles Governing Photometry (1983), Pavillon de Breteuil, F-92310 Sevres, France, p. 12.

2. CIE (International Commission on Illumination), The Basis of Physical Photometry, Publication CIE No. 18.20 (1983).

3. R. L. Booker and D. A. McSparron: Photometric Calibrations, NBS Special Publication 250-15 (1987).

4. T. M. Goodman and P. J. Key: The NPL Radiometric Realization of the Candela, Metrologia **25**, 29-40 (1988).

5. L. P. Boivin, A. A. Gaertner, and D. S. Gignac: Realization of the New Candela (1979) at NRC, Metrologia **24**, 139-152 (1987).

6. G. Eppeldauer: Long-term changes of silicon photodiodes and their use for photometric standardization, Appl. Opt. **29**, 2289 (1990).

7. G. Eppeldauer and M. Racz: Compact Self-Calibrating Setup for High Sensitivity Absolute Light Measurements, in Transactions, Twentieth CIE Session, Amsterdam, Holland, (1983) 1, paper E19/1-3.

8. G. Eppeldauer: Temperature Dependent Inversion Layer Photodiode Self-Calibration, in Proceedings, Twelfth International Symposium on Photon Detectors (IMEKO, Varna, Bulgaria, 1986).

9. G. Eppeldauer and J. E. Hardis: Fourteen decade photocurrent measurements with large area silicon photodiodes at room temperature, Appl. Opt. **30**, 3091 (1991).

10. G. Eppeldauer: High Sensitivity Absolute Radiometer, in Proceedings, Tenth International

Symposium on Photon Detectors (IMEKO, Berlin, FRG, 1982), 145-146.

11. G. Eppeldauer: Measurement of Very Low Light Intensities by Photovoltaic Cells, in Proceedings, Eleventh International Symposium on Photon Detectors (IMEKO, Weimar, GDR, 1984), 182.

12. G. Eppeldauer: Simple Realization of the Radiometric and Photometric Scales, in Proceedings, Tenth IMEKO Congress (IMEKO, Praha, Czechoslovakia, 1985) 4, 208.

13. Methods of Characterizing the Performance of Radiometers and Photometers, CIE Publication No. 53 TC-2.2 (1982) 3.

14. G. Eppeldauer: Temperature-monitored/controlled silicon photodiodes for standardization, SPIE proceedings 1479, Int. Symposium on Optical Engineering and Photonics in Aerospace Sensing, Orlando, FL (1991), 71.

15. E. F. Zalewski, NBS Measurement Services: The NBS Photodetector Spectral Response Calibration Transfer Program, NBS Special Publication 250-17, (1988), 42 and 45.

16. C. L. Cromer, G. Eppeldauer, J. E. Hardis, T. C. Larason, and A. C. Parr: The NIST Detector-Based Photometric Scale, Submitted to Applied Optics.

17. C. Cromer: A New Spectral Response Calibration Method Using a Silicon Photodiode Trap Detector, Proceedings of the Measurement Science Conference, Anaheim, CA, (1991).

18. Methods of Characterizing Illuminance Meters and Luminance Meters, Publication CIE No. 69 (1987) 9.

19. J. H. Walker, R. D. Saunders, J. K. Jackson, and D. A. McSparron: Spectral Irradiance Calibrations, NBS Special Publication 250-20 (1987).